Targeting of Mammalian Glycans Enhances Phage Predation in the Gastrointestinal Tract

Sabrina I. Green[1], Carmen Gu Liu[1], Xue Yu[1], Shelley Gibson[2], Wilhem Salmen[1], Anubama Rajan[1], Hannah E. Carter[1], Justin R. Clark[1], Xuezheng Song[3], Robert F. Ramig[1], Barbara W. Trautner[4,5], Heidi B. Kaplan[6], Anthony W. Maresso[1#]

Address correspondence to Anthony Maresso, maresso@bcm.edu.

[1]Department of Molecular Virology and Microbiology, Baylor College of Medicine, Houston, TX, USA

[2]Department of Human Genetics, Baylor College of Medicine, Houston, TX, USA

[3]Department of Biochemistry, Emory Comprehensive Glycomics Core, Emory University School of Medicine, Atlanta, GA, USA.

[4]Michael E. Debakey Veterans Affairs Medical Center, Houston, TX, USA.

[5]Department of Medicine, Baylor College of Medicine, Houston, TX, USA.

[6]Department of Microbiology and Molecular Genetics, McGovern Medical School, University of Texas Health Science Center at Houston, Houston, Texas, USA.

Key Words

Phage therapy, *E. coli*, multidrug-resistance, bacteriophages, pathogen, pathobiont

Abstract

The human mucosal surface is a complex ecosystem comprised of a eukaryotic epithelium, a prokaryotic microbiota, and a carbohydrate-rich interface that separates them. A less characterized, third entity, that of bacteriophage (phage), parasitizes prokaryotes but generally do not interact with eukaryotic cells. In the gastrointestinal tract, the interaction of these two domains of life influences the health status of the host, especially if there is colonization with invasive pathobionts. If the pathobiont causes a symptomatic infection, treatment with antibiotics is necessary. However, antibiotics act broadly thereby killing many protective commensals and they lack the physio-chemical properties to be optimally active in the mucosa, and may have associated adverse effects, including toxicities. Here, we report a novel C3 type phage of the genus *Kuravirus* whose lytic cycle is enhanced in intestinal environments. The enhanced activity is encoded in the viral tail fiber gene, whose protein product binds human heparan sulfated proteoglycans and localizes the phage to the epithelial cell surface, thereby positioning it near the location of its bacterial host. This finding offers the prospect of developing epithelial-targeting phage to selectively remove invasive pathobiont species from mucosal surfaces.

Introduction

The human mucosal surface is a diverse community comprised of bacteria, viruses, fungi, and human epithelial, immune, and stem cells. The chemistry of the surface is

complex—commonly composed of proteins, lipids, nucleic acid, and small molecule metabolites (Sansonetti, 2004; Nataro, 2005). The pH, ionic environment, and physio-mechano properties also contribute to this dynamic surface. All of these factors influence the biology, and, in turn, disease and treatment. Research over the last decade has revealed the importance of mucosal homeostasis. Invasive pathobionts may colonize, grow, and cause acute or chronic infections, some of which may become systemic and life-threatening (Johnson JR, 2002; Russo and Johnson, 2003). The bacterial composition of this intestinal community varies in association with human illnesses such as cancer, diabetes, neurological illness, obesity, and cardiovascular disease (De Martel *et al.*, 2012; Sampson and Mazmanian, 2015; Maruvada *et al.*, 2017; Vatanen *et al.*, 2018; Tang, Li and Hazen, 2019).

Antibiotics have revolutionized medicine. The meteoric rise of multidrug resistance threatens a returns to pre-antibiotic days by 2050 (O'Neill, 2016). In addition, it is increasingly recognized that antibiotics act as a commensal destroying napalm. The antibiotics developed commercially have focused on inhibition of key processes common to all bacterial species, for example, the inhibition of protein or cell wall biosynthesis. Current antibiotics lack the specificity to selectively target a causative pathobiont, which in the mucosal environment, might be the major driver of the disease among the backdrop of hundreds of benign, even beneficial, symbionts. Moreover, the core chemical backbones of antibiotics (e.g. β-lactam antibiotics) somewhat limit the ability to develop new modified versions. Furthermore, these modifications improve enzymatic activity (e.g. increase affinity or induced suicide inhibition) but has not

enhanced the drug's activity in the human mucosal environment. Mucosal-active, targeted drugs that specifically control the bacterial composition of this complex environment without perturbing ecological balance would promote the health of the nasopharyngeal, lower respiratory, gastrointestinal, and urogenital epithelium.

The rise of multidrug resistance has precipitated the search for alternative antibacterial approaches, including the use of bacteriophages (phages) which are bacterial viruses used to treat infections. Although phage therapy has been used in Eastern Europe for decades, only in the past few years has it been employed for compassionate use cases in the U.S. and Europe and in clinical trials (Schooley *et al.*, 2017; Dedrick *et al.*, 2019; Jault *et al.*, 2019). In theory, phage offer numerous advantages over antibiotics, including that they can be specific towards a given species of bacteria resulting in potential microbiome sparing, "generally regarded as safe or GRAS attributes, allowing them to be given in high doses, and diverse, as phage mixtures can be used to either broaden the range or reduce the frequency of resistance or both (Loc-Carrillo and Abedon, 2011; Grose and Casjens, 2014; Moye, Woolston and Sulakvelidze, 2018). However, their greatest attribute has been speculated to be their abundance – estimated to be 10^{31} on Planet Earth. The phage genosphere—all the collection of genes and their unique biology—sometimes referred to as "viral dark matter", may encode novel features that allow for enhanced lytic activity towards bacterial pathogens (Youle, Haynes and Rohwer, 2012; Brum *et al.*, 2016; Terwilliger *et al.*, 2020). Reasoning that this genosphere may include phage with unique phenotypes that facilitate lytic activity against pathobionts at mucosal environments, we report here a

novel podovirus of the genus *Kuravirus* that infects pathogenic *E. coli* using positional targeting to human heparan-sulfated proteoglycans.

Results

The gastrointestinal tract is prohibitive to phage therapy

Escherichia coli are gram-negative bacilli found in a variety of environments, including the human intestinal microbiome, with > 90% of people colonized (Mitsuoka, Hayakawa and Kimura, 1975). Although most strains are benign, *E. coli* is particularly troubling because of its propensity to undergo horizontal transfer of genes encoding virulence factors and antimicrobial resistance (Huang *et al.*, 2001; Antão, Wieler and Ewers, 2009; Price *et al.*, 2013; Mathers, Peirano and Pitout, 2015; Poole *et al.*, 2017). Thus, several pathotypes have arisen that are associated with human disease. InPEC (Intestinal pathogenic *E. coli*) are associated with diarrhea and gastroenteritis. ExPEC (Extraintestinal pathogenic *E. coli*) are associated with systemic infections of the urinary tract, brain, peritoneum, peripheral organs, blood, and in-dwelling devices, resulting in 9 million infections per year (Russo and Johnson, 2003; Colpan *et al.*, 2013; Poolman and Wacker, 2016). The pandemic ExPEC sequence type 131 or ST131 possess a rare combination of multidrug resistance and enhanced virulence (Pitout, 2012; Johnson *et al.*, 2013; Banerjee and Johnson, 2014). These strains readily colonize the human intestine, which can become a reservoir, prior to extraintestinal infection (Nicolas-Chanoine, Bertrand and Madec, 2014). Previous studies reported that phage HP3, a

lytic myovirus isolated from environmental reservoirs of ExPEC, could reduce ST131 bacteremia and disease severity in murine models of infection (Green *et al.*, 2017a; Ma *et al.*, 2018). Since the human gastrointestinal tract is the primary reservoir of ExPEC ST131, we wondered if phage HP3 could act prophylactically to reduce or eliminate ExPEC burden in the intestine. To test this, mice were orally gavaged with an ExPEC ST131 clinical isolate then treated with phage or an antibiotic as illustrated in Figure 1A. Untreated mice sustained stable bacterial colonization during the course of the experiment (6 days) (Figure 1B). When phage HP3 were given to animals via water or a daily gavage, the levels of ExPEC were indistinguishable from the untreated control at the end of the experiment. However, no ExPEC was detected at any time point in the antibiotic-treated group. Interestingly, phage HP3 was detected, and active, in the stool of phage-treated mice, even on day 4, indicating the lack of ExPEC reduction was not due to a lack of delivery to the intestinal environment or to inactivation of the phage (Figure 1C). It should also be noted that despite having higher levels of phage upon gavage during days 1-4, the phage was no more effective at removing ExPEC than phage given in the water, suggesting that in this experiment there was no dose dependent effect of phage. In addition, as much as 10^5 (PFU/g) phage were found in the murine intestinal tissue (including cecum and colon) on day 6, the final day of the study, yet there was little to no clearing of ExPEC compared to the untreated control in these tissues (Figures 1D and 1E). Importantly, antibiotic treatment significantly reduced the number of operational taxonomic units (OTUs) and diversity, as determined by the Shannon diversity index, which takes into account species richness and distribution (Figure 1Fi, ii). Also, a Principle component analysis (PCA) of beta diversity

demonstrated that mice in the antibiotic cohort clustered together and away from the untreated and phage groups, suggesting antibiotics had a more profound effect on the microbiome than did phage (Figure 1Fiii). Finally, we assessed phage killing in a modified “cecal medium” or CM that is derived from the murine cecal contents and designed to simulate the luminal complexity of the mammalian intestine (Figure 1G). Whereas phage HP3 completely abolished ExPEC in LB (nearly a 9-log drop in levels and no detectable live bacteria), and nearly abolished it in a slurry of fecal pellets taken from the same murine host (~ 8-log drop in levels), there was little to no phage-based killing in CM, despite recovering nearly 10^6-$10^{7.5}$ PFU/mL (Figures 1H and 1I) of phage. The result was the same when the experiment was repeated anaerobically (data not shown). These results mirrored those from the ExPEC colonization model and indicate there is/are factor(s) present in the mammalian gastrointestinal tract that inhibit even the best of lytic phages.

Figure 1

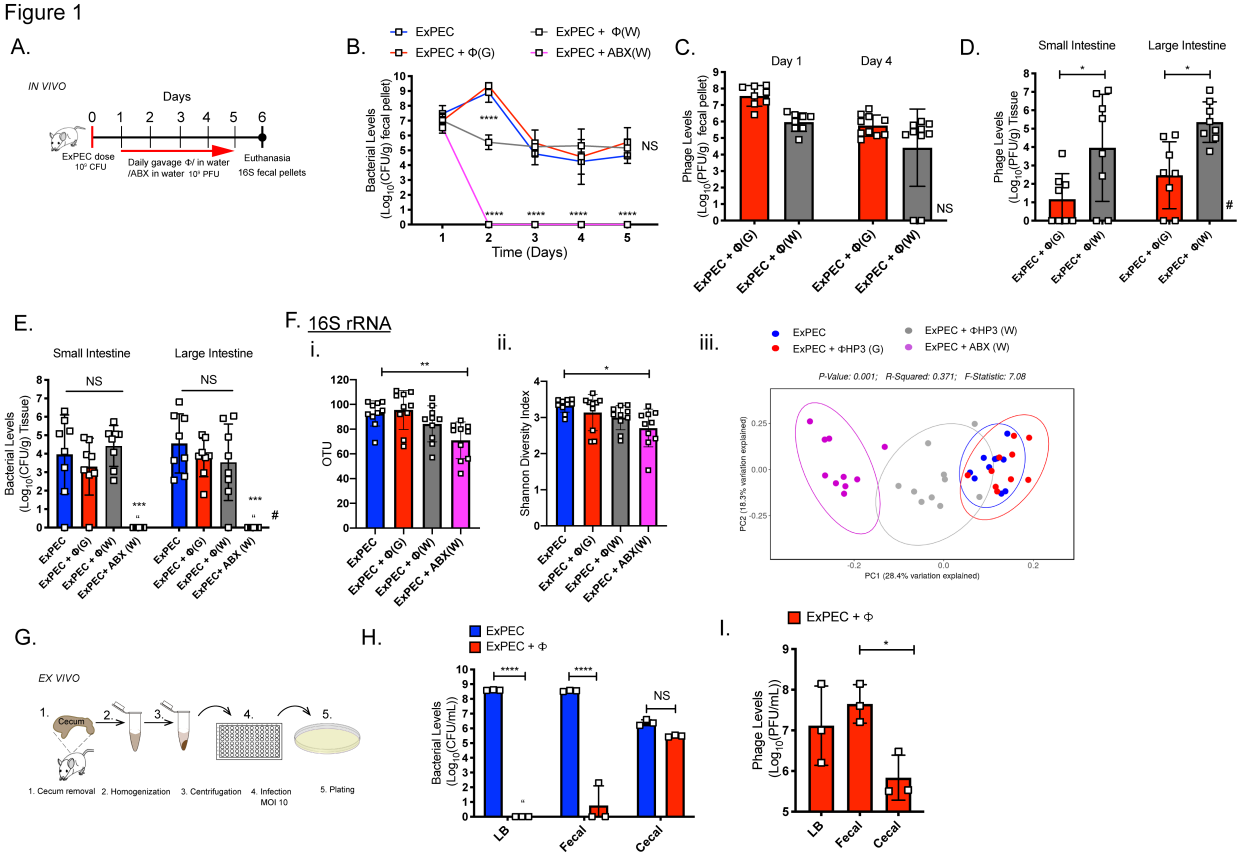

Figure 1: The gastrointestinal tract is prohibitive to phage therapy

(A) Mice (BALB/c) were gavaged with ExPEC ST131 on day 0. Starting on day 1 mice were gavaged (daily) with phage HP3 or given phage or antibiotic (ampicillin) in water and euthanized on day 6. (B) Intestinal (fecal) colonization of ExPEC (C) and phage HP3 levels. (D) From day 6, Intestinal (tissue) HP3 levels and (E) ExPEC levels. (Fi) OTU values of 16S rRNA analysis of fecal pellets from day 6. (Fii) Shannon diversity values (Fiii) Principle component analysis showing beta diversity (N=8-10) (G) Cecal medium (CM) development. (H) ExPEC levels after 4.5 hours growth and (I) phage HP3 levels. (N=3) *p = 0.05, *** p < 0.001, **** p < 0.0001, NS not significant," = none detected, # missing values due to tissue histological analysis of 2 mice/group. Mean, ±SD shown.

The inhibitory component is mucin

We used CM to investigate why phage HP3 was ineffective in this intestinal microenvironment. Previously, we had shown that phage HP3 utilizes calcium for efficient infection, suggesting the effect may be nutritionally-based (Ma *et al.*, 2018). However, addition of calcium did not increase phage HP3 killing in CM (data not shown). We next tested whether the inhibition might be related to the presence of live bacterial microbiota in CM. However, ExPEC killing with phage was not enhanced with removal of the microbiota with a broad range of antibiotics, including inhibitors of protein synthesis, cell wall, and DNA synthesis (Figure S1i-iii – note that the antibiotics efficiently killed a commensal, antibiotic-sensitive, *E. coli* that was spiked into the CM, iv). Furthermore, the inhibitory effect was maintained when a related, and equally as effective phage EC1 was used in the same experiment, thereby indicating the inhibitory effect was not solely due something specific for phage HP3 (data not shown). Arriving at no resolution as to what the inhibitory factor may be, we decided to test more drastic treatments for their ability to restore phage killing in CM. First, the CM was heat-treated (Figure 2Ai, HT CM). Interestingly, heat treatment led to greater than a 6-log improvement in ExPEC killing by phage HP3 (Figure 2Aii). Similarly, when CM was filter-treated (Figure 2Ai, FT CM), there was no detectable levels of ExPEC in the medium after treatment with phage HP3 (Figure 2Aiii), and, this observation was extended to another phage showing inhibition in CM, EC1 (Figure S2A). Thus, the inhibitory component was large (retained on 0.22 micron filter) and sensitive to boiling.

We reasoned intestinal mucins might fit this profile due to their highly associative and sticky properties (captured on a filter) and as proteins they would be sensitive to heat. Mucins are extensively glycosylated proteins found throughout the gastrointestinal system, which form a layer between the intestinal epithelial cells (IECs) and the commensal or pathogenic microbiota (Johansson and Hansson, 2016). Also, they can function as receptors for microbes (McGuckin *et al.*, 2011). To test whether mucins were inhibiting bacterial killing by phage, we devised another method whereby CM was separated via high speed centrifugation into soluble (S CM) and insoluble (INS CM) forms (Figure 2Bi). We hypothesized that INS CM would contain mucin, since large intestinal mucins are normally present in this portion, and be inhibitory to phage killing, whereas the S CM would not have these properties (Carlstedt *et al.*, 1993). Indeed, phage killing in unprocessed CM or INS CM was inhibited to a greater extent than in S CM (Figure 2Bii). To more directly test the hypothesis that mucin was the inhibitory factor, the mucolytic drug N-acetyl cysteine (NAC) was added to INS CM and porcine gastric mucin (1.5 % m/v) added to S CM (Figure 2Bi-ii). Indeed, a 5-log reduction in phage killing of ExPEC was observed in INS CM upon addition of NAC, which also improved killing to that seen in S CM (****$p<0.0001$). Perhaps more compelling, the addition of mucin to S CM abrogated bacterial killing by phage to levels originally observed in CM alone. These results indicate that the inhibitor of phage killing in cecal medium is intestinal mucin.

Figure 2

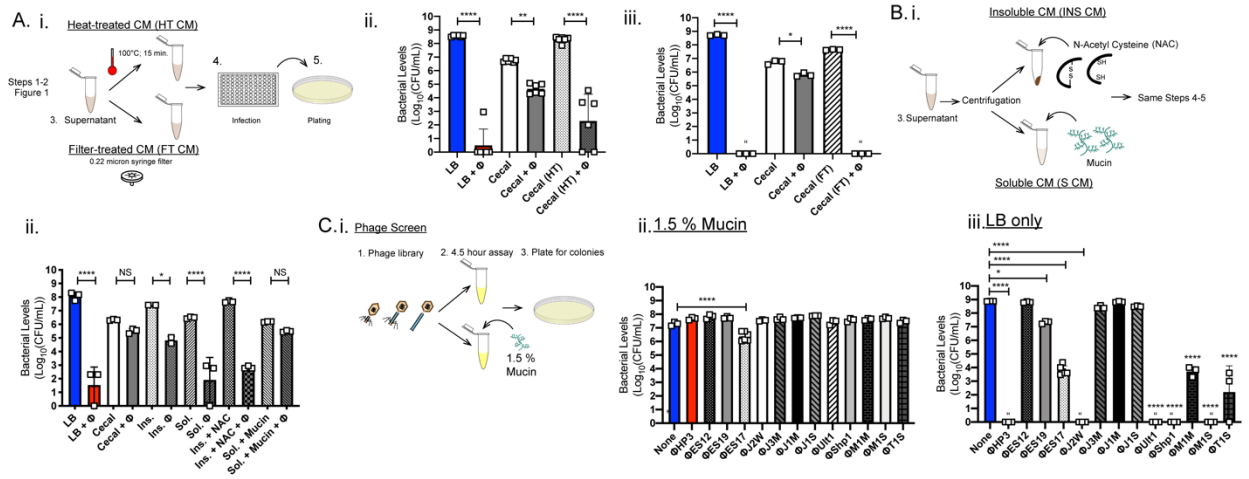

Figure 2: The inhibitory component is mucin. (Ai) CM was heat-treated (HT, 100°C) or filter treated (FT) prior to assay. (Aii) ExPEC levels in HT CM. (Aiii) ExPEC levels in FT CM. (Bi) CM following high speed centrifugation was separated into pellet (insoluble), homogenized and treated with N-acetyl cysteine (NAC), or into supernatant (soluble) and mucin added. Following assay modified CM was plated for (Bii) ExPEC levels. (Ci) A screen of phage killing in mucin was performed using the phage in Table 1. (Cii) ExPEC levels in LB and 1.5% mucin. (Ciii) LB alone. N=3-6, *p = 0.05, *** p < 0.001, **** p < 0.0001, NS not significant, “ = none detected. Mean, ±SD shown.

Along these lines, *E. coli* is known to use mucins as a source of carbon (Chang *et al.*, 2004). We reasoned that a murine host colonized with ExPEC may see a bloom upon NAC treatment due to the drug liberating the mucins for bacterial consumption and thus serve as a system to test if the reduction in aggregated mucin would promote phage HP3’s ability to kill ExPEC. Indeed, upon treatment with NAC for two weeks, ExPEC levels in the small intestine were increased and phage HP3 reduced ExPEC levels, 2.5 logs, in the small intestine (Figure S2Bi-ii). A similar trend was observed in the large

intestine, but it was not substantial (<1 log reduction), though in both organ sections the data were not significant (Figure S2Biii). The less pronounced effect in the large intestine may be due to the thickness of mucus, and thus the lower likelihood for NAC to be effective at breaking up this mucus. Also, NAC's known to be rapidly absorbed in the small intestinal tissue, thereby losing its effect in the more distal large intestine (Aruoma *et al.*, 1989; Tsikas *et al.*, 1998).

Discovery of a mucin-enhanced phage

An estimated 10^{31} phages exist in nature. And the human gastrointestinal tract contains a large diversity consisting of $>10^{10}$ phages many of which are just beginning to be discovered (Shkoporov and Hill, 2019; Sausset *et al.*, 2020). Reasoning that human sewage or the feces of animals may contain phage that have evolved to target their host in high mucin environments, such as the intestinal tract, we screened our phage library (Gibson *et al.*, 2019) and other phages (Table 1) recently isolated from these environments for enhanced activity in LB containing 1.5% mucin (Figure 2C). This is the same concentration that prevented phage HP3 activity in soluble cecal medium and was shown to provide strong inhibition in LB for up to 8 hours (Figure S3A). Surprisingly, only a single phage, designated phage ES17, significantly killed bacteria in the LB mucin medium (Figure 2Cii, ****$p<0.0001$, about 1-log improvement). Surprisingly, phage ES17 was active in mucin despite being much less effective (> 3-logs) than phages HP3, J2W, Ult1, Shp1, or M1S, which completely killed ExPEC to undetectable levels in LB medium alone (Figure 2Ciii, LB). Consistent with these data, when the

amount of mucin was varied from 0 to 2% and phages HP3 and ES17 were compared for lytic activity against ExPEC, phage HP3 was highly effective as the concentration of mucin was lowered to below 0.5%, but completely inhibited above that level (Figure S3B). However, phage ES17 was most effective at concentrations in which HP3 was inactive (0.5 – 1% mucin) and least active at concentrations below or above this range. Taken together, these data suggests that phage ES17 harbors unique properties that facilitate its ability to efficiently be lytic in the presence of mucin.

Phage ES17 is a rare C3 type phage whose activity is enhanced by mucin.

We sought to understand the nature of phage ES17's enhanced ability to find and lyse its bacterial host in mucin. Phage ES17 was determined to be a dsDNA virus of the order *Caudovirales*, family *Podoviridae* and genus *Kuravirus*. The genus *Kuravirus* was named for the River Kura in Tbilisi, Georgia where the original phage of this genus, PhiEco32, which shows close genetic similarity to ES17, was first isolated (Figure S4A) (Savalia *et al.*, 2008). Kuravirus phages have similar morphological characteristics (Ren *et al.*, 2019), including an elongated C3 type capsid, which is considered a rare morphotype for phages (only 13% of tailed phages have elongated heads) and short tail fibers (Ren *et al.*, 2019). Electron microscopy confirmed ES17 to have these same morphological characteristics (capsid >100 nm – Figure 3A). Similar to other phages of this genus, ES17 has a small genome size consisting of 75,007 bps with 123 predicted ORFs (Figure 3B).

In order to determine why this phage is distinct from other phages that lack activity in mucin-rich environments, we examined the ability of phages ES17 and HP3 to adsorb to their *E. coli* hosts. Previous data had shown that 98% of HP3 was adsorbed in 10 minutes, whereas only 32% of ES17 was adsorbed in that time (Gibson *et al.*, 2019). We wondered whether the addition of mucin could improve phage ES17 adsorption and inhibit the adsorption of phage HP3. A modified adsorption assay was utilized for this experiment using ExPEC "coated" with mucin. Briefly, the bacteria were incubated in different concentrations of mucin (0%-1.5%), pelleted, and washed to remove any mucin that did not adhere to the bacterial surface (Figure 3Ci). Next, a standard adsorption assay was conducted with phages ES17 and HP3. Interestingly, phage ES17 showed no adsorption to ExPEC in 10 minutes in the absence of mucin; however, if first incubated with 1.5% mucin, adsorption increased to 98% (Figure 3Cii). In contrast, 98% of phage HP3 was adsorbed without mucin and the adsorption dropped to 75% in its presence (Figure 3Ciii). Transmission electron microscopy (TEM) analysis of these samples at 10 minutes demonstrated that only in the presence of mucin was phage ES17 found bound to the bacterial surface (red arrows) (Fig 3Di-vi, 4 out of 11 images of ExPEC + mucin had visible evidence of ES17 compared to 0 out of 10 in the absence of mucin). TEM imaging of phage HP3 adsorption showed the presence of bound phage in images with and without mucin present (red arrows) (Figure S4Bi-ii). In this case, 5/14 of the imaged fields showed phage HP3 bound with mucin-coated ExPEC compared with 7/14 bound without mucin (Figure S4Biii). Finally, we adapted an ELISA-like approach to determine if phage ES17 preferred binding to surfaces coated with mucin, a hypothesis consistent with our data. Indeed, when mucin was bound to an

ELISA plate, phage ES17 bound to the mucin-surface at higher levels than phage HP3 (Figure 3E, **p=0.002 and ****p<0.0001). Taken together, using three different approaches, these data obtained suggests that phage ES17 binds mucin, a property that may enhance its ability to infect *E. coli* in mucin-rich environments.

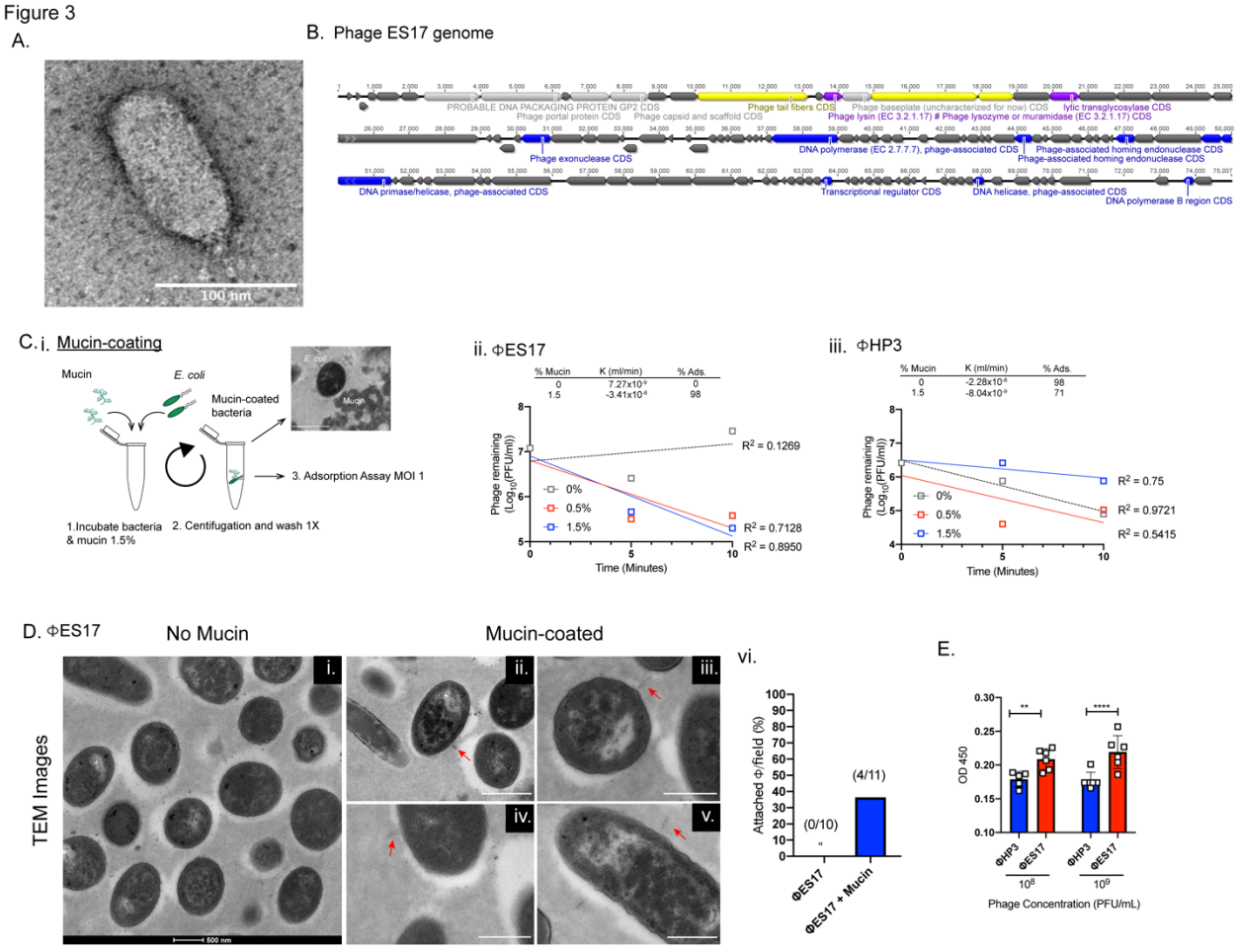

Figure 3: Phage ES17 is a rare C3 type phage with avidity for mucin. (A) TEM image of phage ES17. (B) Genomic organization of ES17. (Ci) ExPEC ST131 was incubated in 0%, 0.5% and 1.5% mucin. Post-centrifugation, bacteria was washed and incubated with phage (MOI 1) for an adsorption assay. (Cii) Phage ES17 and (Ciii)

Phage HP3 adsorption. Adsorption constant (K) and % adsorbed (% Ads.) in 10 min indicated. Regression line generated from mean values of phage remaining for time points indicated. (Di-v) TEM images of phage ES17 and ExPEC fixed after 10 minutes adsorption. White bar scale is 500 nm. Red arrows indicate phage (Dvi) Attached phages per field view. (E) ELISA results for phages HP3 and ES17 on mucin coated plates. N=6, **p < 0.01, *** p < 0.001. " = none detected. Mean, ±SD shown.

Phage ES17 may bind bacterial polysaccharides

As indicated above, phage ES17 is a close relative of the kuravirus phiEco32 and annotated as the same phage type. ES17's putative tail fiber protein (ES17-TFP) showed high homology (64% identical) to a tail fiber protein in another lytic podophage, the T7-like bacteriophage LM33_P1, which also targets ST131 strains (Dufour *et al.*, 2016). This homology is in the C-terminal receptor binding region (Figure S5Ai). The N-terminal region is similar to vB_EcoP_WFI101126 (47% identical), a phage with C3 like morphology similar to phage ES17 (Figure S5Aii)(Korf *et al.*, 2019). The T7-like phage tail fibers have recently been characterized and shown to have knob-like tips, which we also observed in the EM images of phage ES17 (Figure 3A) (Garcia-Doval and van Raaij, 2012). T7-like phage tail fibers have been shown to possess endosialidases that target surface sugars, such as capsule-forming polysaccharides (Garcia-Doval and van Raaij, 2012). A BLAST analysis revealed that ES17-TFP contains a putative pectinesterase (E value 7.45e-03, 369 bp) with high homology to phage lyases (Figure 4A). Modeling of the predicted structure of ES17-TFP indicated it may contain a pectin

lyase fold (Figure S5B, IPR011050). These lyases cleave bacterial polysaccharides and are found in biofilm-degrading phages (Latka *et al.*, 2017). Additionally, this enzyme was not found in phage HP3. Thus, we formed the hypothesis that ES17 might degrade and infect biofilms.

ExPEC is a primary cause of catheter-associated UTI (CAUTI), often associated with the formation of biofilms on the catheter (Russo and Johnson, 2003). For this study, we used a clinical isolate (DS515) from a CAUTI patient, which forms significant biofilms *in vitro* (data not shown). We tested the effect of various *E. coli* phages on DS515 biofilms using a colorimetric assay with a metabolic substrate, MTT, to determine the sensitivity of the biofilm bacteria to the phage (Figure 4B). As determined in Figure 4C, of the 10 *E. coli* phages assessed, which were shown to be lytic towards the clinical isolate, only three phages reduced *E. coli* viability after establishment of the biofilm, and only one of these three, ES17, reduced the biofilm by more than half. Since phage HP3 showed moderate levels of killing of *E. coli* in biofilms, we compared its ability to phage ES17 over a 6-log titration range. Strikingly, as little as 10^3 PFU/ml of phage ES17 statistically reduced biofilm viability, which was greater than that achieved with 10^9 PFU/ml of phage HP3 (Figures 4Di-ii). In addition, phage ES17 showed a dose dependent response at each concentration with the greatest effect seen at 10^9 PFU/ml (****$p<0.0001$) (Figure 4Dii). Also, we found that phage ES17 formed large plaques with halos on DS515 and related clinical isolates (picture above Figure 4Dii). This is in contrast to phage HP3 which showed no halo formation (picture above Figure 4Di). This

halo formation is often indicative of EPS (extracellular polymetric substance)-degrading activity (Knecht, Veljkovic and Fieseler, 2020).

We reasoned ES17-TFP may be responsible for the cleavage of the EPS in the biofilm, thereby allowing phage ES17 to gain access to *E. coli* in the biofilm. Thus, we cloned the DNA encoding ES17-TFP into an expression vector and purified it from *E. coli*. A highly induced band of the expected molecular weight of ES17-TFP (107 KDa) was observed upon SDS-PAGE separation of the eluted fractions (Figure S5C). This band was not observed in the vector only control elutions (data not shown). When ES17-TFP was added to the biofilms, no change in bacterial viability was observed, nor did it enhance ES17 killing of *E. coli* in biofilms when added separately (Figure 4E). Likewise, when incubated in CM, or examined for its ability to degrade mucus using a gel-shift assay in an anti-mucin Western blot, it did not enhance ES17 activity or degrade mucus (data not shown). Furthermore, phage ES17 by itself also did not demonstrate this activity. These data suggests that phage ES17's unique killing abilities are not dependent on degradation of polysaccharides (e.g. mucin or bacterial). This leaves open the question of how this tail fiber protein may enhance killing in carbohydrate-rich environments.

Figure 4

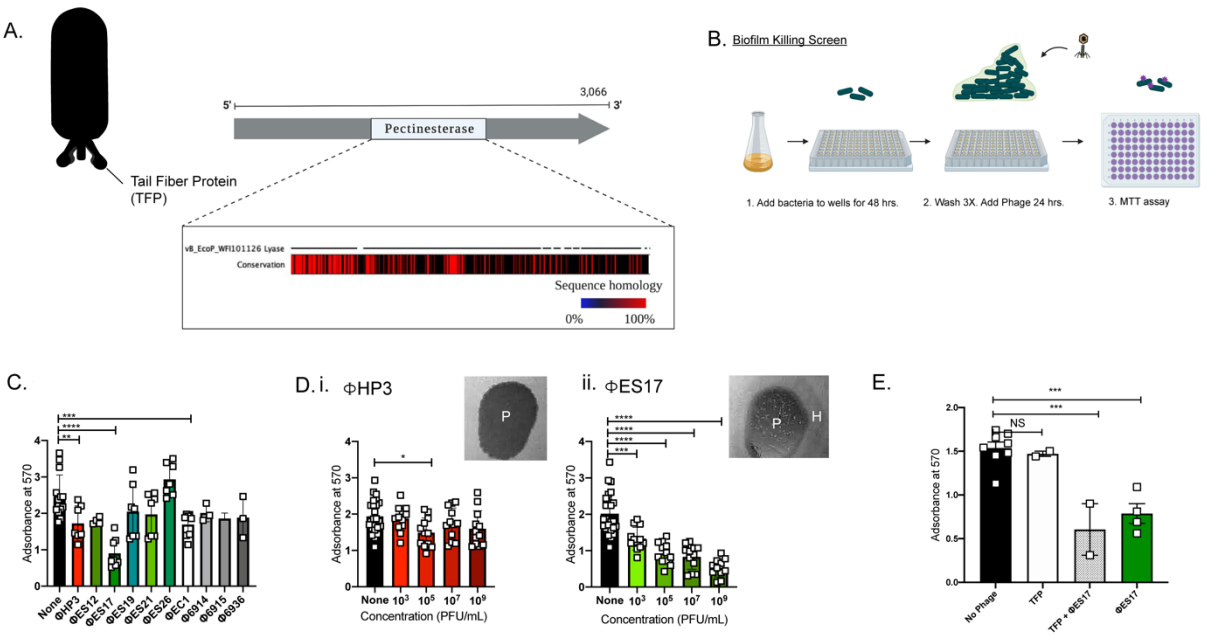

Figure 4: Phage ES17 may bind bacterial polysaccharides. (A) ES17 tail fiber domain (pectinesterase) compared to vB_EcoP_WFI101126 lyase. Red indicates high homology. (B) DS515 was grown overnight in TSB and inoculated in a 96 well plate for 48-hour biofilm growth. A phage library was screened and MTT assay used to quantitate biofilm forming bacteria. (C) DS515 levels with phage library screen (N=3-8). (Di) DS515 levels with phages HP3 and (Dii) ES17 (N=12). Plaques (P) from phages on DS isolate pictured with or without halo (H) (E) ExPEC levels with purified ES17-TFP in CM assay (N=2-8). *p = 0.05, *** p < 0.001, **** p < 0.0001, NS not significant, “ = none detected. Mean, ±SD shown.

Phage ES17 binds human heparan sulfated proteoglycans.

Phage ES17 harbors an enhanced ability relative to other *E. coli* phages to find its bacterial host in environments in which carbohydrates are a prominent chemical component (examples from above include cecal medium, mucin-rich broth, and biofilms). A structural analysis of modeled ES17-TFP showed a high similarity to a phage K5 lyase binding domain (E-value=4E-12). The predicted structure of ES17-TFP (blue) and K5 lyase are pictured in Figure S6Ai (PDB:2X3H; red) with identical residues colored yellow. Phage K5 binds K5 capsular polysaccharide and acts as a K5 polysaccharide lyase (Hanfling *et al.*, 1996). The K5 *E. coli* capsule is made of a repeating disaccharide that is identical to the precursor of heparin and heparan sulfate (HS), a linear polysaccharide, present in glycosaminoglycans (HSPGs, heparan sulfate proteoglycans). (Figure S6Aii) These proteoglycans are found on mammalian cells and in mucus (Monzon, Casalino-Matsuda and Forteza, 2006). Also, mucins with similar structures to heparan sulfate/heparin (α-linked GlcNAC or N-Acetyl-D-glucosamine) are present intestinally and found in PGM (Fujita *et al.*, 2011).

We reasoned that ES17's enhanced activity might be due to a novel ability to bind mammalian polysaccharides found on glycoproteins, which would account for its enhanced activity in a mucin-rich environment and in EPS biofilms. To test this idea, we assessed the ability of purified ES17-TFP to bind to a glycan array containing over 1,000 unique glycan structures, porcine gastric mucin (PGM), glycosaminoglycans (GAGs) and a variety of synthetic and naturally sourced glycans generated by the Consortium for Functional Glycomics (CFG) (see supplementary methods). No or very low relative fluorescent units (RFU), a proxy for binding, was observed for a wide array

of mammalian glycans, including those purified from porcine gastric mucin (Figure S6Bi-ii). However, surprisingly, there was an increase of several orders of magnitude in RFU (RFUs > 2000) observed for binding to the GAGs containing heparan sulfate (ID # 64-173), but not the structurally similar GAGs hyaluronic acid #1-20 or chondroitin sulfate #21-63 (Figure S6Bii-iii). The finding that purified ES17-TFP binds human heparan sulfated proteoglycans provides a possible mechanism to explain why phage ES17 demonstrates enhanced activity in intestinal environments.

ES17 binds to the surface of human intestinal enteroids (HEIMs)

Human intestinal enteroids (HIEs) are organotypic, higher-order cultures that have become popular as surrogates to model the human intestine. They can be grown as 3-dimensional structures complete with a lumen and crypt/villus axis or as 2-dimensional monolayers that facilitate host-pathogen interactions (In *et al.*, 2016; Saxena *et al.*, 2016). These cultures are also useful because they express a variety of glycans found in the human intestine, including mucins and proteoglycans (Saxena *et al.*, 2016). Human intestinal enteroid monolayers (HEIMs) were derived from colonic stem cells following differentiation for 5 days in high Wnt medium. Phage ES17 or HP3 were added to confluent HIEMs for 1 hour, extensively washed, and visualized by immunofluorescence microscopy using antibodies raised against each phage. Little to no detectable phage HP3 was observed on the HIEMs intestinal epithelial cell (IEC) surface, though antibodies generated robust signal and specificity towards the phage when HP3 was fixed on slides alone (Figure 5A and S4C). Phage ES17 (green) bound

evenly to the IECs on the apical side, including areas where prominent Muc2 (red) localization was observed, but also on areas where there was no muc staining (Figure 5Aii). In order to determine whether phage ES17 bound to the IECs of HIEMs via heparan sulfate, we pre-treated the HIEMs with heparinase III to enzymatically remove HSPGs and then assessed phage binding. Indeed, HIEMs treated with heparinase significantly reduced the levels of bound ES17, both qualitatively and quantitatively (Figures 5Bi-vii,****$p<0.0001$). Next, we tested whether this binding to the epithelial cell surface also improved bacterial killing. Previous data had shown that ExPEC adheres less to intestinal enteroids compared to the diarrhea-causing pathogen Enteroaggregative *Escherichia coli* (EAEC) (data not shown). EAEC adheres to HIEMs robustly in an aggregative, mesh-like pattern and similar to phage ES17 utilizes heparan sulfate as a receptor to bind these human colonic cells (Rajan et al., 2020, paper in review)(Poole, Rajan and Maresso, 2018; Rajan *et al.*, 2018). Thus, EAEC serves as an ideal *E. coli* strain to test the hypothesis that phage targeting HSPGs can increase killing. For this experiment we pre-coated HIEMs with phage ES17, washed, as detailed above, then infected with EAEC strain 042. HEIMs were fixed and stained using a Geimsa-Wright stain to visualize cells and bacteria, as previously described (Rajan *et al.*, 2018). Infected HEIMs showed robust bacterial adhesion to cells with an aggregative phenotype (Figure 5Cii, red arrows). Phage coated HEIMs, however, showed significantly reduced EAEC on the surface of the organoid (Figure 5Ciii-iv, **$p<0.01$). Taken together, these data suggests phage ES17 may localize to both the mucus layer and to the IEC surface by binding to HSPGs, which likely position the

phage to be in the exact location needed to find its bacterial target in the intestinal microenvironment.

Figure 5

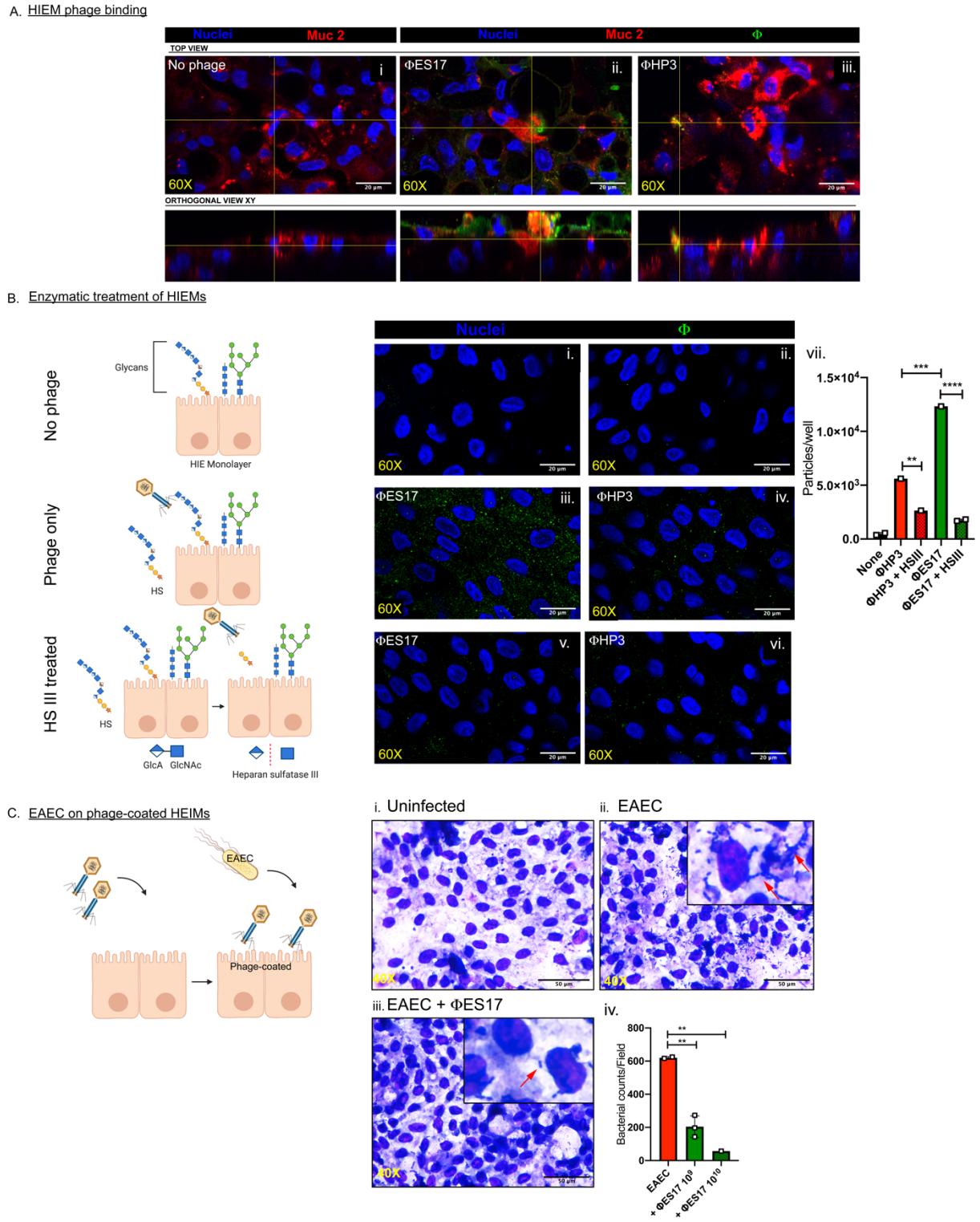

Figure 5: ES17 binds to the surface of human intestinal enteroids (HEIMs). Differentiated HEIMs were incubated with phage for 1 hr, washed, then fixed and imaged for phage (Alexa Fluor 488, Green), intestinal cells (DAPI, Blue), and muc2 (Alexa Fluor 594; Red). (Ai) No phage added. (Aii) ΦES17 and (Aiii) ΦHP3 added. Monolayers were treated with heparanase III then incubated with phage. (Bi, ii) Untreated. (Biii) Phage ES17 and (Biv) phage HP3 added. (Bv) Heparanase treated enteroids incubated with ES17 and (Bvi) HP3. (Bvii) Quantification of particles (phage) per well. (N=1-2). Images were taken at 60X with scale bars shown at 20 μm. HEIMs were (Ci) uninfected or (Cii) Infected with EAEC 042 (Ciii) or pretreated with bacteriophage ES17 prior to infection with EAEC. Images were collected at 60X. The scale bars shown at 50 μm. (Civ) Quantification of EAEC attached to HIEM's per field view. **$p < 0.01$, *** $p < 0.001$, **** $p < 0.0001$. Mean, ±SD shown.

Phage ES17 kills ExPEC in the mammalian intestine

The finding that phage ES17 demonstrated enhanced lytic activity in the presence of mucins, was the best of several screened phages in a mock luminal environment rich in mucins, and binds the human organotypic culture IECs via HSPGs, which leads to EAEC-killing on the bacterial surface, prompted an examination into whether this phage could overcome the intestinal-induced inhibition of phage lytic activity towards colonized ExPEC that was observed for phage HP3. We first tested if ES17 was effective in cecal medium. Indeed, phage ES17 showed a 2.5-log improvement in ExPEC removal in this environment compared to phage HP3 (Figure 6A, ****$p<0.0001$). There was no effect on

the number of OTUs or the Shannon diversity index in this experiment, suggesting phage ES17 was highly selective at removing only the target ExPEC strain (Figure 6Bi-ii). We next tested the effect of phage ES17 on ExPEC in a murine intestine. Animals were colonized with ExPEC as in Figure 1A and treated with either phage ES17 or HP3 (Figure 6C).The dose of phage was also increased from 10^9 PFU to 10^{10} to also evaluate if giving more phage would improve HP3's ability to reduce ExPEC, especially in more proximal segments as the phage slowly moves through the alimentary canal. Examination of the small and large intestine on day 6 showed phage levels were high across all groups (10^6-10^8 PFU/g intestinal tissue) (Figure 6D). Animals treated with phage HP3 had no detectable CFU in small intestinal tissue (Figure 6E), but had indistinguishable levels from that of the untreated control in the cecum. In contrast, every animal treated with phage ES17, except one, had no detectable levels of ExPEC in either the small or large intestine, suggesting that this lytic phage possess a unique ability to target ExPEC in complex mucosal environments such as the large intestine.

Figure 6

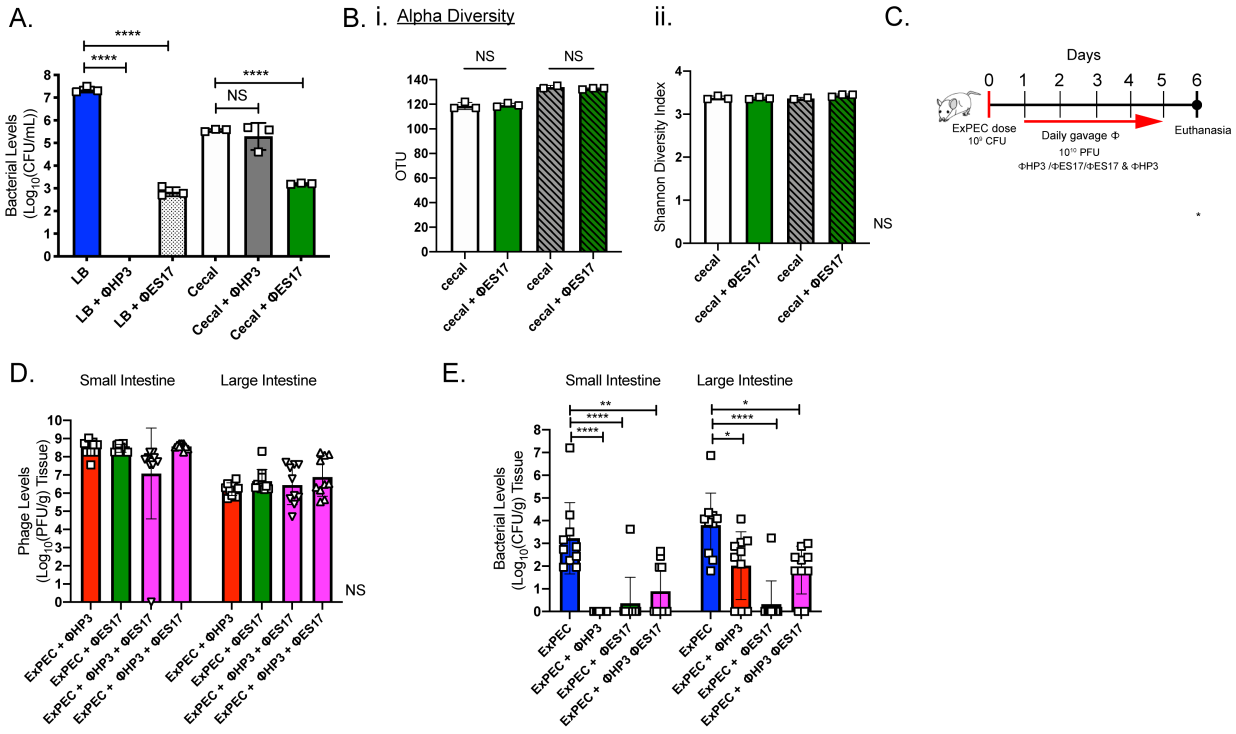

Figure 6: ES17 kills in the mammalian intestine. (A) ExPEC levels in CM assay with ES17 (N=3). 16S rRNA analysis of CM including (Bi) OTU and (Bii) Shannon diversity index. (C) Mice were gavaged with ExPEC then treated with no phage or gavaged daily doses of phage HP3 at 10^{10} PFU, or ΦES17 at 10^{10} PFU or both phages ($2x10^{10}$ PFU total). (D) Intestinal (tissue) phage levels (E) Intestinal (tissue) ExPEC levels. (N=10) *p = 0.05, *** p < 0.001, **** p < 0.0001, NS not significant. “ = none detected. Mean, ±SD shown.

Discussion

A limitation of all antibiotics is their broad killing activity and no inherent features to function well in complex human environments, including human blood, urine, or at mucosal surfaces throughout the body. In particular, the gastrointestinal tract (GIT) is a highly complex system made up of diverse organs and tissues and within that a diversity of cell types. Some of the cells and factors found at the mucosal surface may influence intestinal capacity including: intestinal epithelial cells, enteroendocrine cells, stem cells, mucus-secreting goblet cells, antimicrobial peptides (AMPs – from Paneth cells) and secretory immunoglobulin A (Mammarappallil and Elsinghorst, 2000; Johansson, Larsson and Hansson, 2011; Sato *et al.*, 2011; Gribble and Reimann, 2016; Pickard *et al.*, 2017). To add to this complexity, the GIT is colonized by a large number of microbes—archaea, fungi, protists and bacteria that have co-evolved with the host, termed the human gut microbiota (Pickard *et al.*, 2017; Heintz-Buschart and Wilmes, 2018). A bacteriophage would have to navigate through this complex ecosystem to find and infect its host. Since there are estimated to be $>10^{10}$ PFU/g of phages already present in the GIT, this suggests that phages can thrive in this environment (Hoyles *et al.*, 2014; Shkoporov *et al.*, 2018). Here, we report a novel anti-bacterial targeting strategy that seems to have evolved to position a lytic bacteriophage in the exact niche as its bacterial host. Our results indicate that; (i) phage HP3 that is lytic towards *E. coli* ST131 *in vitro* and is very effective at eliminating bacteremia in a murine model of sepsis, is ineffective when tested for this same property in the murine intestinal tract; (ii) that the inhibition is due to intestinal mucins; (iii) a medium designed to mimic the

luminal environment can be used to identify phage with enhanced lytic activity in such an environment; (iv) a rare C3 type phage, isolated from human wastewater, overcomes this inhibitory activity due to an enhanced ability of the phage to bind to heparan-sulfated proteoglycans present in mucus or immobilized on the surface of intestinal epithelial cells, which likely drives the positional targeting of the phage to the exact ecological niche as the host bacterium. In addition, our data reveal that this treatment when compared to antibiotic treatment, did not alter the intestinal diversity of the microbiota. Taken together these data suggest and that such a phage might also be highly useful for the killing of bacteria in intestinal environments and biofilms, both of which would be desirable properties of a targeted, specific antibacterial.

Potential narrow or limited ecological range of bacteriophages has not been as explored as much as their narrow host range capabilities. Using an experimental process of elimination, we determined that mucin can greatly inhibit phage infection. Mucins are composed of tandem repeats of serine and threonine that act as an attachment sites for o-linked glycans (N-acetlygalactosamine, N-acetylglucosamine, fucose, galactose and sialic acid) (McGuckin *et al.*, 2011; Wang and Hasnain, 2017). Gel-forming mucins, which make up the mucus intestinal layer are large polymers (up to 40 MDa) of mucins attached via disulfide linkages (McGuckin *et al.*, 2011). When we incubated phages with porcine gastric mucin, composed of the gel-forming mucin MUC 5AC (Sturmer *et al.*, 2018), we saw reduced or no bacterial killing. However, when we added N-acetyl cysteine (NAC), which is known to exert a mucolytic effect by reducing the disulfide bonds that keep these mucin polymers together, bacterial killing was restored (Aruoma

et al., 1989; Sadowska *et al.*, 2006). NAC is a drug has been tested and used in the clinical setting to treat syndromes including cystic fibrosis (CF) and chronic obstructive pulmonary disease (COPD). In both of these cases it loosens thick mucus in lungs, but it can also serve as a treatment for acetaminophen overdose due to its antioxidant action (Sadowska *et al.*, 2006; Saito, Zwingmann and Jaeschke, 2010; Bear, 2013). Perhaps this drug could also be used as an adjuvant to phages to help treat patients with bacterial infections in mucin-rich ecosystems such as the gut or the lungs of CF patients. We tested oral NAC treatment in mice and found it to be more effective in improving phage-mediated bacterial killing in the small intestine, but not in the large intestine. NAC has been shown to be rapidly absorbed following oral dosing after only 60 minutes (Tsikas *et al.*, 1998). An oral dose of NAC has a short half-life of 2.5 hours and 10% bioavailability in the gut (Tsikas *et al.*, 1998). It is likely that NAC did not exert a mucolytic effect on the distal large intestine. Interestingly, we observed elevated ExPEC levels in intestinal tissue with NAC treatment. It is possible that some pathogens like ExPEC may thrive in environments with a reduced mucus layer.

Another possibility, distinct from adjuvating phage with NAC, would be to search for phages that have evolved phenotypes that enhance their ability to encounter their bacterial host in a specific ecosystem, such as the GIT. Phage ES17, originally isolated from human sewage, is a member of the family *Podoviridae* and has a rare C3 type elongated capsid morphology with paddle-like short tail fibers (Ackermann, 2001). Previously, this phage was shown to be similar to PhiEco32, a rare Kuravirus which are known for their prolate head (Gibson *et al.*, 2019). Phage ES17 showed a significant

killing effect in cecal medium (CM) and in a mouse model of intestinal colonization compared to phage HP3. Phage ES17 bound mucin significantly better and coating bacteria with mucin increased phage adsorption. There is precedence for this concept. The bacteriophage adhering to mucus (BAM) model proposes that phages bind to mucus via *hoc* proteins or Ig (immunoglobulin fold-like) domains present on the capsid proteins of phages similar to T4 (Fraser *et al.*, 2006; Barr *et al.*, 2013, 2015). This mechanism was suggested to explain how phages bind to the metazoan mucosal surface and increase the probability of encountering a bacterial host, likely via a unique type of controlled diffusion that increases spurious interactions with its bacterial target (Barr *et al.*, 2013, 2015). These studies showed that T4 adsorption increased in the presence of mucin from 65% to 80% absorbed phage within 10 minutes (Barr *et al.*, 2015). The adsorption changes in phage ES17 in the presence of mucin were all or nothing from 0% to 98% within 10 minutes. This suggests that mucin may be a type of "bridge receptor" for phage ES17 since this phage is ineffective at killing in the absence of mucin, even at very high levels of phage. Such a model would make sense in the context of *E. coli* embedded in a mucin matrix, perhaps breaking down mucin as a source of carbon and thus binding it, thereby allowing the phage to adapt a capsular polysaccharide binding mechanism to structurally related sugars that are prominent on proteoglycans.

Bacteriophages have been shown to have a variety of carbohydrate-binding proteins present on tail fibers in order to bind different sugars present on the bacterial cell surface (Nobrega *et al.*, 2018). Some of the most diverse are capsular depolymerases,

which bind and break down capsular carbohydrates secreted by bacteria (Pires *et al.*, 2016). These capsular depolymerases are diverse because of the diversity of bacterial capsule types. Capsule types have been shown to mimic some components of the intestinal system, including sugars present in the mucus layer (Vimr and Lichtensteiger, 2002; Severi, Hood and Thomas, 2007). Bacteria can use these mechanisms to subvert the immune system and to allow for the colonization of hosts (Vimr and Lichtensteiger, 2002; Kahya, Andrew and Yesilkaya, 2017). Phage ES17 was effective at killing bacteria in biofilms and possessed a protein with putative capsular depolymerase domains in a tail fiber protein. However, we could not detect any polysaccharide lyase activity and instead detected strong and stable affinity for a human intestinal sugar, the glycosaminoglycan sugar, heparan sulfate. This suggests a model whereby phage ES17 adapted to “colonize” the mucosal environment by binding to mammalian sugars. Heparan sulfate proteoglycans (HSPG) are expressed on the surface of many types of cells and prominently on the surface of intestinal epithelial cells (Garcia *et al.*, 2016). One of the more tantalizing discoveries here was that human enteroids derived from colonic stem cells specifically bound phage ES17, but not other *E. coli* phages. HSPGs consist of repeating units of sulfated polysaccharides—heparan sulfate (HS). HS is a linear polysaccharide that begins as the precursor, heparan (disaccharide of α1,4-linked N-acetylglucosamine (GlcNAc) and β1,4-linked glucuronic acid (GlcUA)) (Sugahara and Kitagawa, 2002; Murphy *et al.*, 2004). Subsequent modifications due to sulfation and epimerization leads to the mature form polysaccharide HS (Murphy *et al.*, 2004). Bacteriophage K5 utilizes a tail spike lyase (*KflA*) to bind and degrade K5 capsule present on *E. coli* strains (Hanfling *et al.*, 1996). Because the K5 capsule (heparoson;

β1,4-linked GlcUA and α1,4-linked GlcNAc) polysaccharide has been shown to be structurally identical to heparan sulfate precursor, heparan, this enzyme can also act a heparinase (Hanfling *et al.*, 1996; Roberts, 1996; Murphy *et al.*, 2004; O'Leary, Xu and Liu, 2013). K5 heparan lyase cleaves the linkage of N-acetyl glucosamine and glucuronic acid, but is inhibited by sulfated regions (Murphy *et al.*, 2004; O'Leary, Xu and Liu, 2013). Further homology searches showed that the carbohydrate binding domain found in ES17-TFP is structurally homologous to the binding domain present in the tail spike in phage K5. Considering that heparanase III cleaves at the same regions where K5 lyase would bind and degrades suggests ES17-TFP is utilizing the same receptor. Indeed, the addition of heparanse III, from the soil bacteria *Flavobacterium heparinum*, which specifically cleaves unmodified (unsulfated) NAc domains (GlcNAc-GlcUA) and NA/NS domains (GlcNS (N-Sulfo-D-Glucosamine) and GlcNAc) of HS, leads to abrogated phage ES17 binding to cells, meaning ES17 was highly specific for this type of glycan (Murphy *et al.*, 2004; Park *et al.*, 2017). Structurally similar mucins to heparan sulfate (Class III type, α-linked GlcNAc) suggest that this protein may also target these intestinal mucins (Ota *et al.*, 1998; Fujita *et al.*, 2011). This interaction is driven by phage ES17's tail fiber protein, which is not related to the *hoc* proteins or contain an Ig-like fold as predicted from the BAM model. Thus, it would seem that phage ES17 uses a novel mechanism to localize not only a mucin-rich surface, but also directly to the mammalian epithelial surface (Figure 7). It is worth speculating that not only would this be a way to intercept *E. coli* that would also colonize this surface, but it could also be exploited therapeutically as a prophylactic "epithelium protecting" coating that prevents the pathobiont from invading the mucosa. Several pathogens, including

bacteria and human pathogenic viruses have been shown to bind to HS and use them as receptors (Alvarez-Dominguez *et al.*, 1997; Fleckenstein, Holland and Hasty, 2002; Cagno *et al.*, 2019). It is tempting to speculate that this property might have been also acquired by phage, as suggested here.

Figure 7

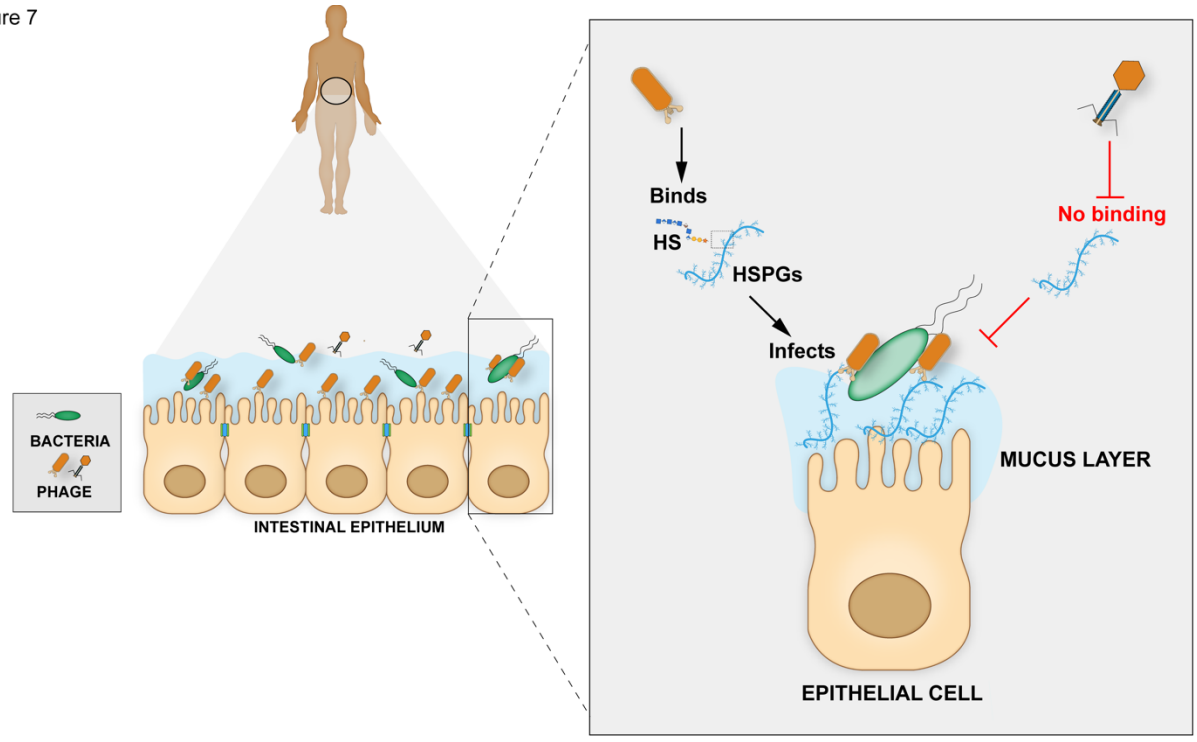

Figure 7: Model showing phage ES17 utilizing its tail fiber to bind polysaccharides present on the bacterial surface of pathogens and mammalian sugars, including heparan sulfate (HS), present on intestinal mucosal surfaces. This binding helps facilitate infection of bacteria in the human gastrointestinal tract, potentially in biofilms as well. Other phages that cannot bind these sugars are inhibited from killing bacteria in these environments. HSPGs (heparan sulfate proteoglycans).

Materials and Methods

Bacterial strains and phages

ExPEC ST131 isolate JJ1901 was used in all ExPEC infections, except Figure S1Aiii (JJ2528). Both isolates were previously obtained from Dr. Jim Johnson (University of Minnesota)(Green *et al.*, 2017b). Commensal *E. coli* ECN (Figure S1iv) was isolated from a human fecal sample. Deidentified strain DS515 is a clinical isolate obtained from the clinical microbiology laboratory at the Houston Veterans Administration Hospital. Prior to infections all strains were grown overnight at 37°C from a single colony streaked on an LB agar plate. The intestinal pathogen EAEC 042 (serotype 44:H18), was originally isolated from a child in Peru, and extensively characterized (Nataro *et al.*, 1985).

Phages HP3, ES12, ES17, ES19, ES21 and ES26 have been previously described and characterized (Green *et al.*, 2017a; Gibson *et al.*, 2019). Phage 6914, 6915 and 6939 were recently isolated from sewage. All phages described in Table 1 were isolated by single plaque isolation from environmental sources as described previously (Green *et al.*, 2017b; Gibson *et al.*, 2019).

Murine infections

Mixed ages (6-10 months) and sexes of BALB/c (Jackson laboratories, Bar Harbor, ME) mice were used in mouse models of infection. Mice were kept in SPF environment at Baylor College of Medicine CCM (Center for Comparative Medicine) Taub facility. For infections mice were kept in a biohazard facility with sterile food and water. The mice were individually housed during colonization experiments and bedding replaced with autoclaved techboard liners for daily fecal collection. For models of ExPEC colonization, mice received a 10^9 CFU dose of ExPEC strain JJ1901 via oral gavage. Rodent health was monitored daily for indication of pain or disease. Colonization (fecal and intestinal) was determined after homogenization and selective plating for the chloramphenicol resistant strain JJ1901 on LB agar plates containing chloramphenicol and colony counting as previously described (Green *et al.*, 2017a). Purified phage in 3% (m/v) $NaHCO_3$ was administered either via gavage or in water 5% (m/v) sucrose added *ad libitum*. All groups received sucrose and $NaHCO_3$ in water for consistency. The antibiotic ampicillin (1g/500 ml) was administered in water. Phage colonization was quantified after dilution of homogenates a serial plating on a double agar overlay assay.

Ex vivo cecal model

A modified cecal assay was used for experiments (Theriot *et al.*, 2014). Briefly, cecal contents from just euthanized mice were pooled and homogenized in sterile 0.09% NaCl solution at a 1:5 dilution (mg:mls). The homogenate was centrifuged to remove large particulates (2000 G for 30 sec.). The supernatant fluid was used for 4.5 hr assays at an MOI of 10 at 37°C, shaking (255 RPM), as previously described (Ma *et al.*, 2018).

For FS CM, cecal supernatant was centrifuged (6000 G for 5 min.) and filtered through a 0.22 μm syringe filter. For HT CM, the supernatant was heated at 100°F for 20 min in a hot water bath, then cooled to RT for infections. Insoluble CM and soluble CM (supernatant) were isolated post high-speed centrifugation (9000 G for 5 min) of CM. The insoluble pellet was resuspended in sterile 0.09% Nacl solution for infections (IN CM). For the mucin assays, porcine gastric mucin type II (PGM; Sigma-Aldrich) was used at various concentrations diluted in phosphate buffered saline (PBS). The mucolytic drug N-acetly cysteine (NAC, Sigma-Aldrich, 5 mg/ml) was diluted in PBS for de-mucolytic assays.

Phage Sequencing and Annotation

The annotation figure was generated from previous data (Gibson *et al.*, 2019) using Geneious Prime 2019.2.3 and adjusted in Inkscape.

Mucin-coating Adsorption and Imaging

For the adsorption curves, assays were performed at an MOI of 1 using mid-log phase cultures and samples taken every 5 min for 10 min. Prior to adsorption, PGM (0%, 0.5% and 1.5% m/v) was added to the bacterial cultures for 10 min. RT, shaking (255 RPM). The cultures were centrifuged (6000 G for 5 min) and gently washed with PBS. The adsorption rate constants (K) were determined from the natural log of the slope of the adsorption curve versus the bacterial concentration. Some cultures were fixed in

glutaraldehyde solution after 10 min adsorption for TEM imaging. TEM imaging was performed at the Texas Children's Hospital Center for Digestive Diseases. After fixation the samples were dehydrated in ethanol and followed by evaporation of ethanol and coating with gold for observation during TEM.

Mucin Binding ELISA Assay

Clear-walled Immulon 2 HB 96-well microtiter plate (Immunochemistry Technologies #227) were used for the ELISA assays. PGM (200 μl of 1mg/ml) was added to a microtiter plate and incubated at 4°C overnight. The next day the mucin was removed and wells were washed twice with PBS. The phage was added to wells for 1 hr then washed three times in PBST (PBS with 0.1% Tween-20). The wells were blocked with BSA then incubated with antibodies for the phage overnight at 4°C. Following washing steps, a HRP (horse radish peroxidase) conjugated antibody was added for 1 hr. To assess phage binding, TMB solution was added until the wells turned light blue and then a stop solution (2M H_2SO_4) was added. The absorbance was read at 450 nm.

Biofilm Screening

Biofilm experiments were recently described but with some modifications (Mapes *et al.*, 2016). *E. coli* DS515 cultures grown in tryptic soy broth (TSB) were diluted to an OD of 0.1 and seeded to inoculate a 96 well plate for the biofilm formation assay. The plates were incubated statically at 37°C for 48 hrs. Following incubation, planktonic cells were

removed, and the wells were washed three times in PBS. Phages diluted in TSB to 10^9 PFU/ml were added and incubated for 24 hrs at 37°C statically. The wells were washed three times in PBS then an MTT assay was performed to determine the metabolic activity of the phage resistant biofilm-forming bacteria. Protein quantification was determined using a Bradford assay (Biorad) using BSA as a standard. Purified ES17-TFP was added at a concentration of 0.17 mg/ml to biofilms with added phage.

HEIM Infection and Imaging

Human enteroid monolayers (HEIMs) were differentiated for 5 days (>90% confluent) as described (Poole, Rajan and Maresso, 2018). For experiments HIEMs were incubated with phage at 10^8 PFU/ml in culture differentiation media for 1 hour at 37°C in the presence of 5% CO_2 in a humidified incubator, then washed in PBS. The HIEMs were fixed in Clark's solution for 10 min to preserve the mucus layer. The HIEMs were permeabilized and blocked with 5% BSA in 0.1% Triton X-100 in PBS for 30 min at RT. Mucus was detected using antibodies to MUC2 (1:200) (Abcam) and nuclei stained with 4′, 6′-diamidino-2-phenylindole (DAPI) (300 nM) for 5 min at RT. Antibodies against phages HP3 and ES17 were generated from whole virus (phage) injection into rabbits performed by Pacific Immunology. A 13 week antibody production protocol consisted of 4 immunizations and anti-sera collection.

To selectively removed HSPG from GAG chains, enteroid cultures were pretreated with heparinase III (Sigma, 2U/ml) for 2 hours, as described (Jiao *et al.*, 2007), followed by the

addition of phage. Images were captured using a Zeiss LSM 510 confocal microscope. Represented images were adjusted equally for brightness and contrast using FIJI software version 2.0.0. The images were adjusted equally for brightness and contrast. Particle analysis was used to determine particles per well. The Cell counter program in FIJI was used to quantitate bacteria (EAEC) per field of view.

EAEC infection and staining

For infection of HEIMs, the EAEC strain 042 was grown overnight and then sub-cultured (1:100) for 2 hrs at 37°C. One microliter of the log-phase bacterial culture was added to 100 microliters of the cell culture media and added to chambered slides either with phage-coated HEIMs (as described above) or untreated. Cultures were incubated for 3.5 hrs at 37°C in the presence of 5% CO_2 in a humidified incubator. Following growth, bacteria were removed, by gently washing the cells in PBS then the remaining cells were fixed (Hema 3 fixative) and stained using a Geimsa-Wright stain (Fisher scientific). The infection and staining technique have been previously described (Rajan *et al.*, 2018).

Statistics

Statistical analysis was performed using PRISM 8 software. For figures with log transformed data and groups >2 significance was determined using a one-way ANOVA

analysis or two way ANOVA when necessary (Figure 3E). For multiple comparison analysis, the secondary test, Tukey, was used. For nontransfomed data a normality test (Shapiro-Wilk) was performed to determine normality before a one-way ANOVA analysis was performed. Unless otherwise stated all graphs show the mean and standard deviation.

Acknowledgements

This work is supported in part by grant from US Veterans Affairs (VA I01-RX002595), Roderick D. MacDonald Research Fund at Baylor St. Luke's Medical Center, the Mike Hogg Foundation, and Seed Funds from Baylor College of Medicine Seed Fund
We would like to thank Dr. Melinda Engevik for general expertise and protocol help related to mucin work. We would also like to thank Hannah Johnson from the Integrated Microscopy Core at Baylor College of Medicine for technical assistance related to imaging.

Author Contributions

S.G., C.L., X.Y., W.S., A.R., H.C. and X.S. performed experiments and analyzed data. J.C. performed bioinformatics studies. R.R., B.T., and H.K., contributed to design of studies and edited the manuscript. S.G. designed studies and wrote the manuscript. A.M. contributed to design and overall major goals of the study and edited the manuscript.

References

Ackermann, H. W. (2001). Frequency of morphological phage descriptions in the year 2000. Arch. Virol. *5*, 843–857.

Alvarez-Dominguez, C. *et al.* (1997). Host cell heparan sulfate proteoglycans mediate attachment and entry of Listeria monocytogenes, and the listerial surface protein ActA is involved in heparan sulfate receptor recognition. Infect. Immun. *1*, 78–88.

Antão, E.-M., Wieler, L. H. and Ewers, C. (2009). Adhesive threads of extraintestinal pathogenic *Escherichia coli*. Gut. Pathog. doi: 10.1186/1757-4749-1-22.

Aruoma, O. I. *et al.* (1989). The antioxidant action of N-acetylcysteine: its reaction with hydrogen peroxide, hydroxyl radical, superoxide, and hypochlorous acid. Free Radic. Biol. Med. 593–597.

Banerjee, R. and Johnson, J. R. (2014). A new clone sweeps clean: The enigmatic emergence of *Escherichia coli* sequence type 131. Antimicrob. Agents CH. *9*, 4997-5004.

Barr, J. J. *et al.* (2013). Bacteriophage adhering to mucus provide a non-host-derived immunity. Proc. Natl. Acad. Sci. *26*, 10771–10776.

Barr, J. J. *et al.* (2015). Subdiffusive motion of bacteriophage in mucosal surfaces increases the frequency of bacterial encounters, Proc. Natl. Acad. Sci. *44*, 13675–13680.

Bear, C. E. (2013). 50 years ago in the Journal of Pediatrics: the effect of N-acetylcysteine on the viscosity of tracheobronchial secretions in cystic fibrosis of the pancreas, J. Pediatr. *1*, 85.

Brum, J. R. *et al.* (2016). Illuminating structural proteins in viral “dark matter” with metaproteomics. Proc. Natl. Acad. Sci. *9*, 2436-2441.

Cagno, V. *et al.* (2019). Heparan Sulfate Proteoglycans and Viral Attachment: True Receptors or Adaptation Bias? Viruses. *7*. 596.

Carlstedt, I. *et al.* (1993). Characterization of two different glycosylated domains from the insoluble mucin complex of rat small intestine. J. Biol. *25*, 18771-18781.

Chang, D. E. *et al.* (2004). Carbon nutrition of *Escherichia coli* in the mouse intestine. Proc. Natl. Acad. Sci. *19*, 7427-7432.

Colpan, A. *et al.* (2013). *Escherichia coli* sequence type 131 (ST131) subclone h30 as an emergent multidrug-resistant pathogen among US Veterans. Clin. Infect. Dis. *9*, 1256-1265.

Dedrick, R. M. *et al.* (2019). Engineered bacteriophages for treatment of a patient with a disseminated drug-resistant Mycobacterium abscessus. Nat Med. *5*, 730-733.

Dufour, N. *et al.* (2016). Bacteriophage LM33_P1, a fast-acting weapon against the pandemic ST131-O25b: H4 *Escherichia coli* clonal complex. J. Antimicrob. *11*, 3072-3080.

Fleckenstein, J. M., Holland, J. T. and Hasty, D. L. (2002). Interaction of an Outer Membrane Protein of Enterotoxigenic *Escherichia coli* with Cell Surface Heparan Sulfate Proteoglycans. Infect. Immun. *3*, 1530–1537.

Fraser, J. S. *et al.* (2006). Ig-like domains on bacteriophages: a tale of promiscuity and deceit. J. Mol. Biol. *2*, 496–507.

Fujita, M. *et al.* (2011). Glycoside hydrolase family 89 α-N-acetylglucosaminidase from clostridium perfringens specifically acts on GlcNAcα1,4Galβ1R at the non-reducing terminus of O-glycans in fastric mucin. J .Biol. Chem. *8*, 6479-6489.

Garcia-Doval, C. and van Raaij, M. J. (2012). Structure of the receptor-binding carboxy-terminal domain of bacteriophage T7 tail fibers. Proc. Natl. Acad. Sci .U S A. *24*, 9390–9395.

Garcia, B. *et al.* (2016). Surface Proteoglycans as Mediators in Bacterial Pathogens Infections. Front. Microbiol. *7*, 220.

Gibson, S. B. *et al.* (2019). Constructing and Characterizing Bacteriophage Libraries for Phage Therapy of Human Infections. Front. Microbiol. *10,* 2537.

Green, S. I. *et al.* (2017a). Bacteriophages from ExPEC Reservoirs Kill Pandemic Multidrug-Resistant Strains of Clonal Group ST131 in Animal Models of Bacteremia. Sci Rep. doi: 10.1038/srep46151.

Gribble, F. M. and Reimann, F. (2016). Enteroendocrine Cells: Chemosensors in the Intestinal Epithelium. Annu. Rev. Physiol. 277–299.

Grose, J. H. and Casjens, S. R. (2014). Understanding the enormous diversity of bacteriophages: The tailed phages that infect the bacterial family Enterobacteriaceae, Virology. *468*, 421–443.

Hanfling, P. *et al.* (1996). Analysis of the enzymatic cleavage (beta elimination) of the capsular K5 polysaccharide of *Escherichia coli* by the K5-specific coliphage: reexamination. J. Bacteriol. *15*, 4747–4750.

Heintz-Buschart, A. and Wilmes, P. (2018). Human Gut Microbiome: Function Matters. Trends Microbiol. *7*, 563–574.

Hoyles, L. *et al.* (2014). Characterization of virus-like particles associated with the human faecal and caecal microbiota. Res. Microbiol. *10*, 803–812.

Huang, S. H. *et al.* (2001). A novel genetic island of meningitic *Escherichia coli* K1 containing the ibeA invasion gene (GimA): Functional annotation and carbon-source-regulated invasion of human brain microvascular endothelial cells. Funct. Integr. Genomic. *5*, 312-322.

In, J. G. *et al.* (2016). Human mini-guts: New insights into intestinal physiology and host-pathogen interactions. Nat. Rev. Gastroenterol. Hepatol. *11*, 633–642.

Jault, P. *et al.* (2019). Efficacy and tolerability of a cocktail of bacteriophages to treat burn wounds infected by *Pseudomonas aeruginosa* (PhagoBurn): a randomised, controlled, double-blind phase 1/2 trial. Lancet Infect. Dis. *1*, 35-45.

Jiao, X. *et al.* (2007). Heparan sulfate proteoglycans (HSPGs) modulate BMP2 osteogenic bioactivity in C2C12 cells. J. Biol. Chem. *2*, 1080–1086.

Johansson, M. E. V. and Hansson, G. C. (2016). Immunological aspects of intestinal mucus and mucins. Nat. Rev. Immunol. *10*, 639–649.

Johansson, M. E. V., Larsson, J. M. H. and Hansson, G. C. (2011). The two mucus

layers of colon are organized by the MUC2 mucin, whereas the outer layer is a legislator of host-microbial interactions. Proc. Natl. Acad. Sci. *108*, 4659–4665.

Johnson, J. R. *et al.* (2013). Abrupt emergence of a single dominant multidrug-resistant strain of *Escherichia coli*. J. Infect. doi: 10.1093/infdis/jis933.

Johnson JR, R. T. (2002). Extraintestinal pathogenic *Escherichia coli:* "The other bad *E coli*". J. Lab. Clin. Med*. 3,* 155-162*.*

Kahya, H. F., Andrew, P. W. and Yesilkaya, H. (2017). Deacetylation of sialic acid by esterases potentiates pneumococcal neuraminidase activity for mucin utilization, colonization and virulence. PLOS Pathog. *3*, doi: 10.1371/journal.ppat.1006263.

Knecht, L. E., Veljkovic, M. and Fieseler, L. (2020). Diversity and Function of Phage Encoded Depolymerases. Front. Microbiol. *10*, 29449.

Korf, I. H. E. *et al.* (2019). Still Something to Discover: Novel Insights into Escherichia coli Phage Diversity and Taxonomy. Viruses. *5*, 454.

Latka, A. *et al.* (2017). Bacteriophage-encoded virion-associated enzymes to overcome the carbohydrate barriers during the infection process. Appl. Microbiol. *8*, 3103-3119.

Loc-Carrillo, C. and Abedon, S. T. (2011). Pros and cons of phage therapy,

Bacteriophage. *2*, 111-114.

Ma, L. *et al.* (2018). Metals Enhance the Killing of Bacteria by Bacteriophage in Human Blood. Sci. Rep.*1,* 2326.

Mammarappallil, J. G. and Elsinghorst, E. A. (2000). Epithelial Cell Adherence Mediated by the Enterotoxigenic *Escherichia coli* Tia Protein, *12*, 6595–6601.

Mapes, A. C. *et al.* (2016). Development of expanded host range phage active on biofilms of multi-drug resistant *Pseudomonas aeruginosa*. Bacteriophage. doi: 10.1080/21597081.2015.1096995.

De Martel, C. *et al.* (2012). Global burden of cancers attributable to infections in 2008: A review and synthetic analysis. Lancet Oncol. *6*, 607-615.

Maruvada, P. *et al.* (2017). The Human Microbiome and Obesity: Moving beyond Associations. Cell Host Microbe. *5*, 589-599.

Mathers, A. J., Peirano, G. and Pitout, J. D. (2015). *Escherichia coli* ST131: The quintessential example of an international multiresistant high-risk clone. Adv. Appl. Microbiol. *90*, 109–154.

McGuckin, M. A. *et al.* (2011). Mucin dynamics and enteric pathogens. Nat. Rev

Microbiol. *4*, 265–278.

Mitsuoka, T., Hayakawa, K. and Kimura, N. (1975). The fecal flora of man, Zentralbl Bakteriol. Orig. A. *4*, 499–511.

Monzon, M. E., Casalino-Matsuda, S. and Forteza, R. M. (2006). Identification of glycosaminoglycans in human airway secretions. Am. J. Resp. Cell. Mol. *2*, 135–141.

Moye, Z. D., Woolston, J. and Sulakvelidze, A. (2018). Bacteriophage applications for food production and processing. Viruses. *2*, 135.

Murphy, K. J. *et al.* (2004). A new model for the domain structure of heparan sulfate based on the novel specificity of K5 lyase. J. Biol. Chem. *26*, 27239–27245.

Nataro, J. P. *et al.* (1985). Detection of an adherence factor of enteropathogenic *Escherichia coli* with a dna probe. J. Infect. doi: 10.1093/infdis/152.3.560.

Nataro, J. P. (2005) *Colonization of Mucosal Surfaces*. Edited by W. N. J. Nataro, James P. Cohen S. Paul, Mobley L.T. Harry. ASM. doi: 10.1128/9781555817619.

Nicolas-Chanoine, M. H., Bertrand, X. and Madec, J. Y. (2014). *Escherichia coli* st131, an intriguing clonal group. Clin. Microbiol. Rev. doi: 10.1128/CMR.00125-13.

Nobrega, F. L. *et al.* (2018). Targeting mechanisms of tailed bacteriophages. Nat. Rev. Microbiol. *12*, 760–773.

O'Leary, T. R., Xu, Y. and Liu, J. (2013). Investigation of the substrate specificity of K5 lyase A from K5A bacteriophage. J. Glycobiol.*1*, 132–141.

O'Neill, J. (2016). Antimicrobial Resistance : Tackling a crisis for the health and wealth of nations, Review on Antimicrobial Resistance.

Ota, H. *et al.* (1998). New monoclonal antibodies against gastric gland mucous cell-type mucins: A comparative immunohistochemical study. Histochem Cell Biol. doi: 10.1007/s004180050272.

Park, H. *et al.* (2017). Heparan sulfate proteoglycans (HSPGs) and chondroitin sulfate proteoglycans (CSPGs) function as endocytic receptors for an internalizing anti-nucleic acid antibody. Sci .Rep.*1*, 14373.

Pickard, J. M. *et al.* (2017). Gut microbiota: Role in pathogen colonization, immune responses, and inflammatory disease. Immunol. Rev. *1*, 70–89.

Pires, D. P. *et al.* (2016). Bacteriophage-encoded depolymerases: their diversity and biotechnological applications. Appl. Microbiol .Biotechnol. *5*, 2141–2151.

Pitout, J. D. D. (2012). Extraintestinal pathogenic *Escherichia coli:* A combination of virulence with antibiotic resistance. Front. Microbiol. doi: 10.3389/fmicb.2012.00009.

Poole, N. M. *et al.* (2017). Role for FimH in extraintestinal pathogenic *Escherichia coli* invasion and translocation through the intestinal epithelium. Infect. Immun. *11*. doi: 10.1128/IAI.00581-17.

Poole, N. M., Rajan, A. and Maresso, A. W. (2018). Human Intestinal Enteroids for the Study of Bacterial Adherence, Invasion, and Translocation. Curr. Protoc. Microbiol. *1*, 55.

Poolman, J. T. and Wacker, M. (2016). Extraintestinal pathogenic *Escherichia coli*, a common human pathogen: challenges for vaccine development and progress in the field. J. Infect. *1*, 6–13.

Price, L. B. *et al.* (2013). The epidemic of extended-spectrum-β-lactamase-producing *Escherichia coli* ST131 is driven by a single highly pathogenic subclone, H30-Rx. mBio. doi: 10.1128/mBio.00377-13.

Rajan, A. *et al.* (2018). Novel segment- and host-specific patterns of enteroaggregative *Escherichia coli* adherence to human intestinal enteroids. mBio. doi: 10.1128/mBio.02419-17.

Ren, H. *et al.* (2019). Genome sequence analysis of Vibrio parahaemolyticus lytic phage Vp_R1 with a C3 morphotype. Arch. Virol. *11*, 2865–2871.

Roberts, I. S. (1996). The biochemistry and genetics of capsular polysaccharide production in bacteria. Annu. Rev. Microbiol. *50*, 285–315.

Russo, T. A. and Johnson, J. R. (2003). Medical and economic impact of extraintestinal infections due to Escherichia coli: focus on an increasingly important endemic problem, Microbes. Infect. *5*, 449–456.

Sadowska, A. M. *et al.* (2006). Role of N-acetylcysteine in the management of COPD, Int. J. Chron. Obstruct. Pulmon. Dis. *4*, 425–434.

Saito, C., Zwingmann, C. and Jaeschke, H. (2010). Novel mechanisms of protection against acetaminophen hepatotoxicity in mice by glutathione and N-acetylcysteine. Hepatology.*1*, 246–254.

Sampson, T. R. and Mazmanian, S. K. (2015). Control of brain development, function, and behavior by the microbiome. Cell Host Microbe. *5*, 565–576.

Sansonetti, P. J. (2004). War and peace at mucosal surfaces. Nat. Rev. Immunol. *12*, 953–964.

Sato, T. *et al.* (2011). Paneth cells constitute the niche for Lgr5 stem cells in intestinal crypts. Nature. *7330*, 415–418.

Sausset, R. *et al.* (2020). New insights into intestinal phages. Mucosal Immunol. 2, 205–215.

Savalia, D. *et al.* (2008). Genomic and Proteomic Analysis of phiEco32, a Novel *Escherichia coli* Bacteriophage. J. Mol. Biol. *3*, 774–789.

Saxena, K. *et al.* (2016). Human Intestinal Enteroids: a New Model To Study Human Rotavirus Infection, Host Restriction, and Pathophysiology. J. Virol.*1*, 43–56.

Schooley, R. T. *et al.* (2017). Development and use of personalized bacteriophage-based therapeutic cocktails to treat a patient with a disseminated resistant Acinetobacter baumannii infection. Antimicrob. Agents Chemother. doi: 10.1128/AAC.00954-17.

Severi, E., Hood, D. W. and Thomas, G. H. (2007). Sialic acid utilization by bacterial pathogens. Microbiology. *9*, 2817–2822.

Shkoporov, A. N. *et al.* (2018). Reproducible protocols for metagenomic analysis of human faecal phageomes. Microbiome. *1*, 68.

Shkoporov, A. N. and Hill, C. (2019). Bacteriophages of the Human Gut: The “Known Unknown” of the Microbiome. Cell Host Microbe. *2*, 195–209.

Sturmer, R. *et al.* (2018). Commercial Porcine Gastric Mucin Preparations, also Used as Artificial Saliva, are a Rich Source for the Lectin TFF2: In Vitro Binding Studies. Chembiochem, *24*, 2598–2608.

Sugahara, K. and Kitagawa, H. (2002). Heparin and heparan sulfate biosynthesis, IUBMB Life. *4*, 163–175.

Tang, W. H. W., Li, D. Y. and Hazen, S. L. (2019). Dietary metabolism, the gut microbiome, and heart failure. Nat. Rev. Cardiol. *3*, 137–154.

Terwilliger, A. L. *et al.* (2020). Tailored Antibacterials and Innovative Laboratories for Phage (Φ) Research: Personalized Infectious Disease Medicine for the Most Vulnerable At-Risk Patients. PHAGE. doi: 10.1089/phage.2020.0007.

Theriot, C. M. *et al.* (2014). Antibiotic-induced shifts in the mouse gut microbiome and metabolome increase susceptibility to Clostridium difficile infection. Nat. Commun. *5*, 3114.

Tsikas, D. *et al.* (1998). Analysis of cysteine and N-acetylcysteine in human plasma by high-performance liquid chromatography at the basal state and after oral administration

of N-acetylcysteine. J. Chromatogr. B. Biomed. Sci. Appl. *1–2*, 55–60.

Vatanen, T. *et al.* (2018). The human gut microbiome in early-onset type 1 diabetes from the TEDDY study. Nature. *7728*, 589–594.

Vimr, E. and Lichtensteiger, C. (2002). To sialylate, or not to sialylate: that is the question. Trends Microbiol. *6*, 254–257.

Wang, R. and Hasnain, S. (2017). Analyzing the Properties of Murine Intestinal Mucins by Electrophoresis and Histology. BIO-PROTOCOL. doi: 10.21769/bioprotoc.2394.

Youle, M., Haynes, M. and Rohwer, F. (2012). Scratching the surface of biology's dark matter. Viruses. doi: 10.1007/978-94-007-4899-6_4.

Tables

Table 1: Properties of *E. coli* phages used in biofilm screen.

Phages	**ΦES12**	**ΦES17**	**ΦES19**	**ΦJ2W**	**ΦJ3M**	**ΦJ1M**	**ΦJ1S**	**ΦUlt1**	**ΦShp1**	**ΦM1M**	**ΦM1S**	**ΦT1S**
Source	Human	Human	Human	Human	Human	Human	Human	Human	Sheep	Rabbit	Rabbit	Pigs
Source location	Sewage	Sewage	Sewage	Sewage	Sewage	Sewage	Sewage	Sewage	Animal facility	Animal facility	Animal facility	Animal facility
Isolation strain	JJ2050	JJ2547	DS104	JJ2528	JJ2528	JJ2528	JJ2528	JJ1901	JJ1901	JJ1901	JJ1901	JJ1901
Plaque size (mm)	0.5	0.5 – 1.0	0.5	0.5	0.5	0.5	0.5	0.5 – 1.0	0.5	0.5	0.5	0.5
Plaque morphology	Clear	Clear, halo	Clear, halo	Clear, halo	Clear	Clear	Clear	Clear	Clear	Clear	Clear	Clear
ST131 lysed (%)[a.]	9/13 (69)	9/13 (69)	11/13 (85)	-	-	-	-	12/13 (92)	12/13 (92)	11/13 (85)	12/13 (92)	10/13 (77)
Accession #	MN508614	MN508616	MN508617	-	-	-	-	-	-	-	-	-

[a.] ExPEC ST131 library of isolates described previously (Gibson et al., 2019).